

## Characterization of Nanostructured SnO<sub>2</sub> Thin Film Coated by Ag nanoparticles

Mo. Ganjali<sup>a,\*</sup>, Ma. Ganjali<sup>a</sup>, A. Hassanjani-Roshan<sup>a</sup>, S. M. Kazemzadeh<sup>a</sup>

<sup>a</sup> Department of Nanotechnology and Advanced Materials, Materials and Energy Research Center (MERC), Karaj, Iran.

---

### ARTICLE INFO

---

#### Article history:

Received 27 Jan. 2014

Accepted 07 Apr. 2014

Available online 15 May 2014

---

#### Keywords:

SnO<sub>2</sub> Nanoparticles

Thin film

Ag nanoparticles

---

### ABSTRACT

Nanostructured SnO<sub>2</sub> thin films were prepared using Electron Beam-Physical Vapor Deposition (EB-PVD) technique. Then Ag nanoparticles synthesized by laser-pulsed ablation were sprayed on the films. In order to form a homogenous coat of SnO<sub>2</sub> on the glass surface, it was thermally treated at 500°C for 1 h. At this stage, the combined layer on the substrate was completely dried for 8 h in the air at room temperature right after the Ag colloidal NPs were sprayed on the tin oxide layer. The crystal structure and surface morphology of thin film were studied by X-ray diffraction (XRD), electron diffraction x-ray (EDX), transition electron microscopy (TEM) and scanning electron microscopy (SEM). The average crystallite size of SnO<sub>2</sub> nanoparticles estimated by XRD was about 9 nm. On the other hand, the SnO<sub>2</sub> NPs with 6 nm size were distributed by the TEM image. The thickness of SnO<sub>2</sub> –Ag layer was measured about 2.48 μm.

---

### 1. Introduction

SnO<sub>2</sub> based on thin film has been extensively studied as gas resistive sensors because of its good sensing abilities that are not available from other metal oxides from both scientific and practical points of view [1]. Nowadays, alcohol sensors are highly demanded for applications including food industry, breath analysis and environmental monitoring. Much effort has been devoted to exploring excellent sensing materials for ethanol detection, from conventional metal oxide thin or thick films [2–4] to recently novel one-dimensional nanostructures including nanorods [5,6], nanowires [7] nanobelts [8], and nanotubes [9].

SnO<sub>2</sub> sensors have many advantages over other sensors, such as high sensitivity at low gas concentrations, low operation temperature, simple design, and low cost of tin sources. However, other problems such as low selectivity and low stability are associated with SnO<sub>2</sub> sensors. These disadvantages may be overcome by using suitable additives, mainly noble metals such as Ag, Pt, Pd, Au, and Ru [10, 11].

A variety of techniques has been used to deposit tin oxide (SnO<sub>2</sub>) thin films, including spray pyrolysis [12], chemical vapor deposition [13], ion-beam assisted deposition, sputtering [14], and sol-gel methods [15]. Among these methods, EB-PVD offers many desirable

---

Corresponding author:

E-mail address: monireh.gan@gmail.com (Monireh Ganjali).

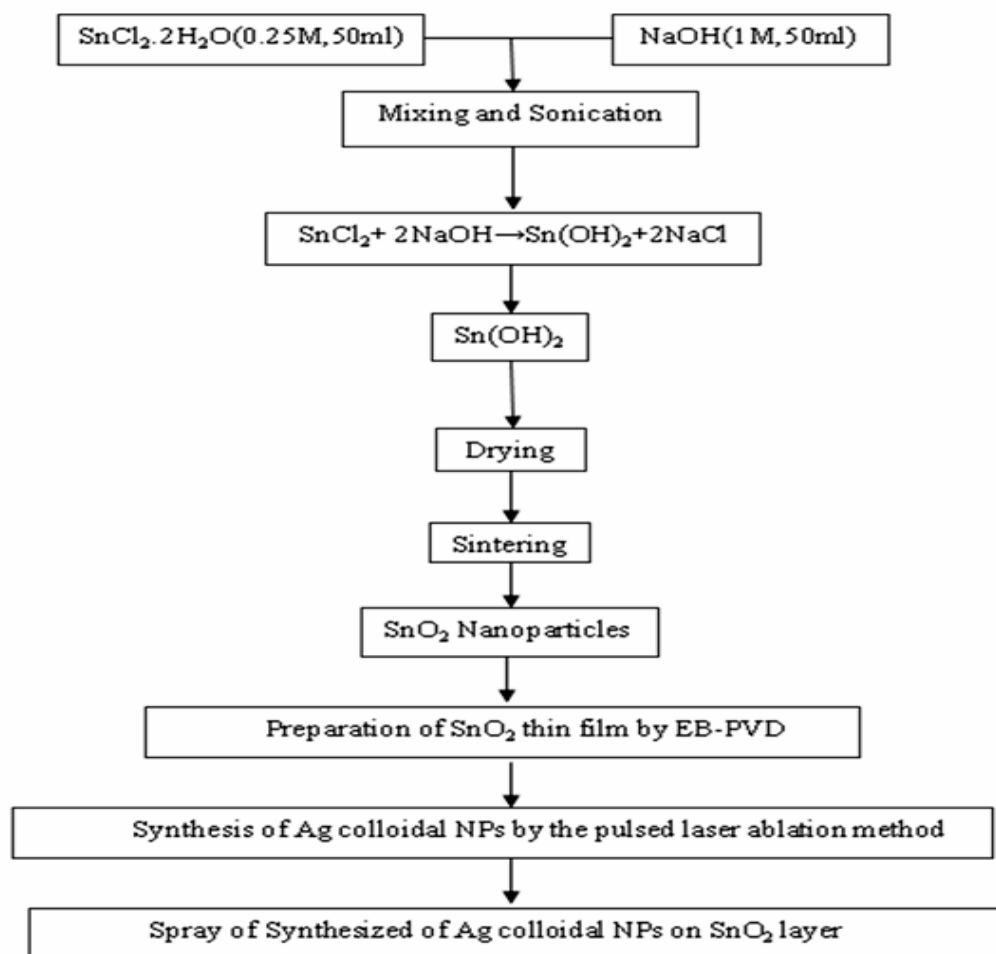


Fig. 1. Flowchart of the experiment design process

characteristics such as flexible deposition rates (1 nm/min up to 100 nm/min, depending on the material, desired microstructure, and property performance), dense coatings, strong metallurgical bonding, tailored composition, columnar and polycrystalline microstructure, and high thermal efficiency [16].

In this work  $\text{SnO}_2$  thin film was prepared using the EB-PVD method. Moreover, after annealing, the uniform clusters began to grow on the  $\text{SnO}_2$  film surface which had been coated smoothly on the glass with addition of Ag NPs.

## 2. Experimental

### 2.1. Materials and equipment

An amount of Tin chloride ( $\text{SnCl}_2 \cdot 2\text{H}_2\text{O}$ , 99.8%, Merck), sodium hydroxide (NaOH, 99.8%, Merck), ethanol ( $\text{C}_2\text{H}_5\text{OH}$ , Merck,

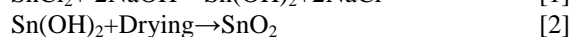
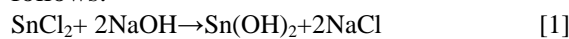
99.99%) and deionized water were used to synthesize the pure nanosized  $\text{SnO}_2$  particles. A high-intensity ultrasonic probe (Misonix S4000, Ti horn, 20 kHz, 100  $\text{W}/\text{cm}^2$ , USA) and a flat-bottomed Pyrex glass vessel (total volume of 150 ml) were used for the ultrasound irradiation. Also, Au plate ( $1 \times 1 \times 1 \text{ cm}^3$ ) and Q-switched Nd:YAG laser (wavelength: 1064 nm, repetition rate: 10 Hz, pulse duration: 10 ns, and fluence  $5 \text{ J} \cdot \text{cm}^{-2}$ ) were used to produce Ag-NPs colloidal NPs. Finally, the Veeco EB-PVD instrument with a pressure of  $5 \times 10^{-6}$  Torr was used for  $\text{SnO}_2$  deposition

The flow chart in fig 1 illustrates the experiment design process:

### 2.2. Synthesis of nano $\text{SnO}_2$ via sonochemical method

NaOH was dissolved in deionized water and

the solution (1 M, 50 ml) was added drop-wise to an aqueous  $\text{SnCl}_2 \cdot 2\text{H}_2\text{O}$  solution that was dissolved in ethanol (0.25 M, 50 ml) within about 30 minutes at a synthesis temperature of 30° C. The reactions between  $\text{SnCl}_2$  and NaOH to form nanosized  $\text{SnO}_2$  particles are as follows:



Sonication of the solution was performed by a Misonix Model S-4000 sonicator through direct ultrasonic irradiation by an immersed Ti alloy ultrasonic horn in the solution.

$\text{SnO}_2$  nanoparticles were prepared by this procedure under the specified conditions with an electric power of the sonicator set at 80 W and temperature set at 30 °C.

During the sonochemical reaction, it was observed that the color of the slurry changed gradually from colorless (before the reaction) into white. These changes of color in the solution occurred as  $\text{SnO}_2$  nanoparticles were prepared. Finally, precipitated particles were collected, filtered and washed carefully with methanol and double distilled water to remove the by-products. All the prepared samples were dried in the air at room temperature for 48 h and then heat-treated at 500 °C for 1 h to obtain crystalline Tin oxide nanoparticles.

### 2. 3. Synthesis of Ag colloidal NPs by pulsed laser ablation method

Ag NPs preparation was carried out by pulsed laser ablation method. It has successfully been reported in our published work with the same experimental condition and optical parameters [17].

Briefly, laser beams were focused on the surface of the silver plate with fluence of 5  $\text{J}/\text{cm}^2$  at the wavelength 1064 nm. It should be noted that silver particles prepared by laser ablation in acetone were stable and free from any precipitates for at least 24 months (without adding any surfactants or other additives).

For generation of smaller Ag nanoparticles with narrow and Gaussian size distribution the ablation was uniformly performed for 30 min after removing the bulk silver target from the solution by the same experimental setup mentioned above.

The effect of laser irradiation was

investigated by measuring optical absorption spectra and TEM images of the colloids taken by transmitting electron microscopy (LEO912AB) with a spectrometer Cary 500 scan.

### 2. 4. Preparation of $\text{SnO}_2$ thin film by EB-PVD

In this research, glass surfaces used as substrates for  $\text{SnO}_2$  deposition were cleaned with ethanol and then rinsed in deionized water and air-dried. Pressed nanopowder  $\text{SnO}_2$  was used as target. The substrate temperature was fixed at 80 °C. The Veeco EB-PVD instrument with a pressure of  $5 \times 10^{-6}$  Torr was used for  $\text{SnO}_2$  deposition. After deposition, the thin film was observed by SEM (VEGA\\TESCAN) working at 25 keV beam energy. Considering the formation of homogenously coated  $\text{SnO}_2$  on the glass surface, it was thermally treated at 500 °C for 1 h. At this stage, the combined layer on the substrate was completely dried for 8 h in the air at room temperature right after the Ag colloidal NPs had been sprayed on the tin oxide layer. Morphology and chemical characterization of the deposited film were analyzed with an SEM (VEGA\\TESCAN) equipped with an EDX.

### 2. 5. Characterization

The crystal structure and the  $\text{SnO}_2$  NPs size were verified by an X-ray diffractometer (Philips PW 3710, Netherlands), using  $\text{Cu K}\alpha_1$  radiation ( $\lambda=1.54 \text{ \AA}$ ). The samples were examined in the  $2\theta$  range from 20°-60° at a scanning speed of 0.04 second/step and a step size of 0.02° in  $2\theta$ .

Morphology of the samples was determined by using transmission and scanning electron microscopies (TEM; ZEISS, Germany and SEM; VEGA\\ TESCAN Czech Republic). TEM samples were prepared by dispersing a few drops of  $\text{SnO}_2$  on carbon films supported by copper grids, and SEM samples were prepared by dispersing a thin layer of the powders on aluminum grids while the surface of each specimen was coated with a thin layer of gold before SEM examination. The SEM analysis was performed at 15 kV. The particle size measurements were carried out by using an Able Image Analyzer v3.6 [20].

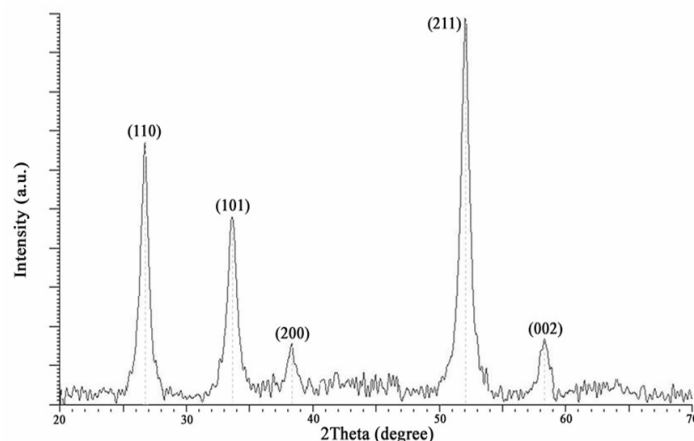


Fig. 2. XRD patterns for SnO<sub>2</sub> NPs synthesized by sonochemical method

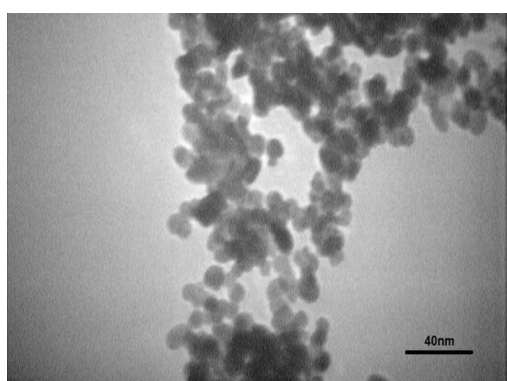


Fig. 3. TEM micrograph of powder prepared by sonochemical method

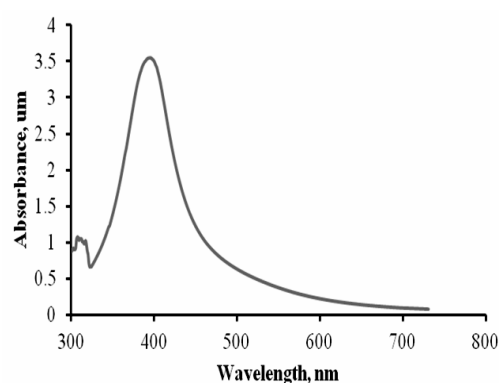


Fig. 4. UV/vis spectra of Ag nanoparticles colloid in acetone solution

### 3. Results and Discussion

#### 3. 1. SnO<sub>2</sub> NPs

Fig. 2 shows the XRD patterns of the SnO<sub>2</sub> NPs synthesized by sonochemical method. The X-ray diffraction peaks of SnO<sub>2</sub> NPs for  $2\theta = 26.8^\circ, 34.05^\circ, 38.12^\circ, 51.9^\circ$  and  $58.25^\circ$  are assigned to (110), (101), (200), (211) and (002), respectively. These results comply with the standard SnO<sub>2</sub> XRD pattern of the JCPDS lines [9]. All diffraction peaks can be readily indexed to tetragonal SnO<sub>2</sub> NPs. No other peaks such as Sn or any other Sn based oxide were observed, which indicates the high purity of the samples. The diffraction peaks are markedly broadened, which indicates that the crystalline sizes of samples are very small.

Due to the spherical shape of the NPs, the average grain size was calculated through the Scherer formula [18]:

$$D = 0.9\lambda/\beta \cos \theta \quad [3]$$

where  $D$  is the average crystallite size,  $\lambda$  is the

X-ray wavelength ( $1.5418 \text{ \AA}$ ),  $\beta$  is FWHM of the peak, and  $\theta$  is the diffraction peak position. The crystallite size of the samples was calculated from the SnO<sub>2</sub> (211) reflection located at  $51.9^\circ$  for different sonicating temperatures. So, the average crystallite sizes of SnO<sub>2</sub> particles determined from Scherrer's equation are about 9 nm, which is consistent with the TEM image (Fig. 3). On the other hand, the SnO<sub>2</sub> NPs with a size of 16 nm were distributed according to the TEM image [20].

#### 3. 2. Colloidal Ag nanoparticles

The UV-vis absorption spectra have been proved to be quite sensitive to the formation of silver colloids because silver NPs exhibit an intense absorption peak due to the surface plasmon excitation that describes the collective excitation of conduction electrons in a metal like Ag [19].

Fig. 4 represents the absorption spectra of the

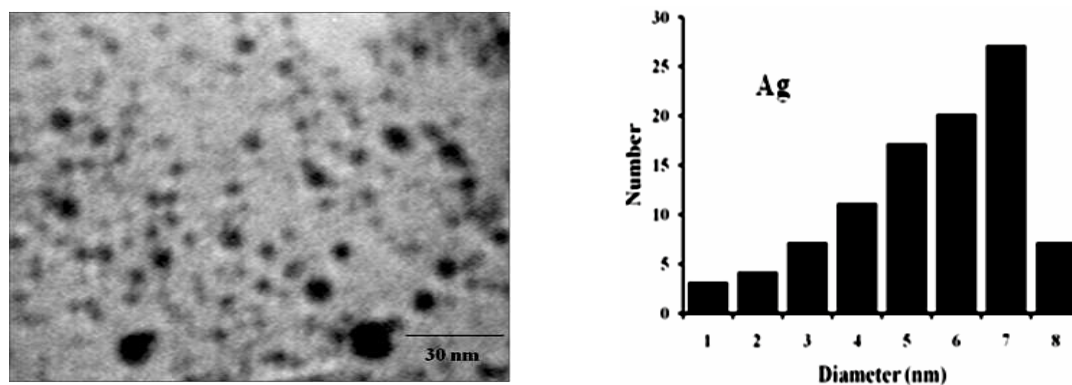


**Fig. 5.** a) TEM micrograph and b) size distribution of the Ag colloidal nanoparticles prepared by Laser-pulsed ablation method in acetone

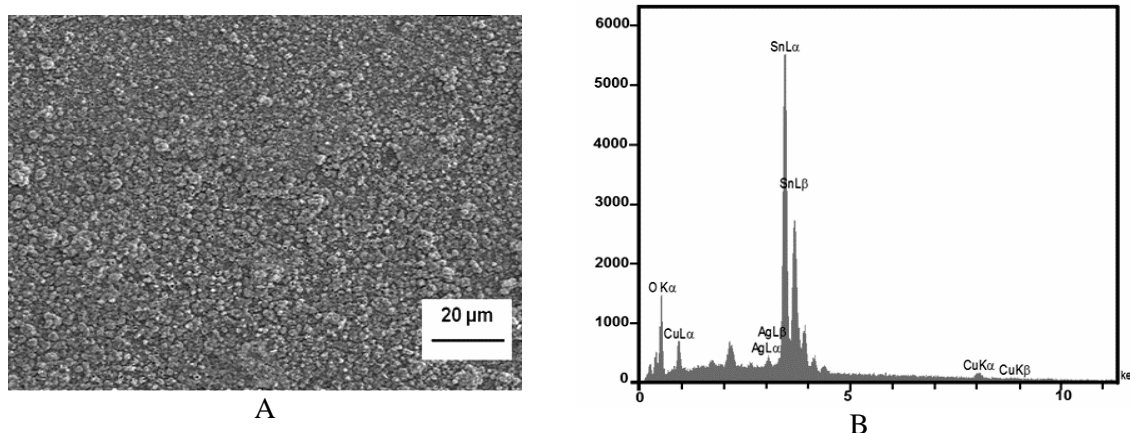


**Fig. 6.** (a) SEM image of the SnO<sub>2</sub> thin films after spraying the Ag colloidal nanoparticles, (b) the corresponding EDX spectra for SnO<sub>2</sub>-Ag film

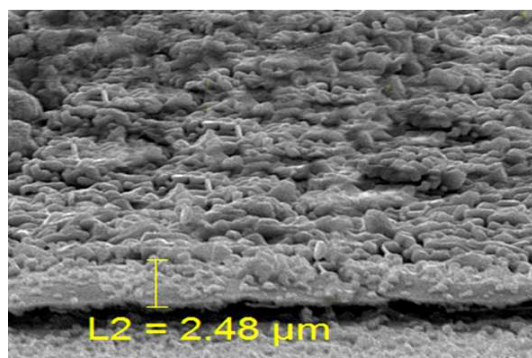


**Fig. 7.** Cross-section of the SnO<sub>2</sub> thin films after spraying the Ag colloidal nanoparticles

Ag nanoparticles produced in acetone solution. The absorption spectrum peak of homogeneously-produced, uniform silver particles by laser-pulsed ablation method is around 400 nm.

The electron micrograph of Ag nanoparticles obtained by TEM is shown in Fig. 5. The

spherical shape of the particles observed by TEM is consistent with the optical absorption peak around 400 nm originated from surface-plasmon excitation.

### 3. 3. SnO<sub>2</sub> thin film

Fig. 6(a) shows the SEM image of SnO<sub>2</sub>-Ag film and fig. 6(b) shows the corresponding EDX spectra. It is clear from fig. 6(a) that the finite size grains are uniformly distributed on the surface of the film. The chemical composition in fig. 6(b), deduced from the EDX measurements, shows major peaks for the bulk substrate material Sn, Ag, and oxygen, and indicates that the film is composed merely of SnO<sub>2</sub>-Ag. Also, a quantity of Cu is present in EDX. The presence of Cu might be due to the use of the Cu tape to attach the samples to the SEM platform. Fig. 7 shows the cross-section image of SnO<sub>2</sub>-Ag film, respectively. From

fig. 6(a) it is clear that the film is dense and exhibits granular structure with a thickness of  $\sim 2.48 \mu\text{m}$ .

#### 4. Conclusions

Nanocrystalline Tin oxide ( $\text{SnO}_2$ ) was synthesized from a suspension containing  $\text{SnCl}_2 \cdot 2\text{H}_2\text{O}$  and aqueous  $\text{NaOH}$  with the aid of ultrasonic irradiation for 30 min.  $\text{SnO}_2$  thin film was deposited on glass substrates by electron beam method. Then the colloidal Ag NPs synthesized by laser-pulsed ablation method were sprayed on the  $\text{SnO}_2$  film. The structure and microstructure evaluations confirm that the synthesized films are nanostructured in nature and the thickness of  $\text{SnO}_2/\text{Ag}$  layer is about  $2.48 \mu\text{m}$ .

#### Acknowledgements

The authors are grateful to the Materials and Energy Research Center (MERC) for extending financial assistance to carry out this work [grant number 728913].

#### References

1. J. Aguilar-Leyva, A. M. de la L Maldonado, "Gas-sensing characteristics of undoped- $\text{SnO}_2$  thin films and  $\text{Ag}/\text{SnO}_2$  and  $\text{SnO}_2/\text{Ag}$  structures in a propane atmosphere", *Materials Characterization*, Vol. 58, 2007, pp. 740 – 744.
2. R. S. Khadayate, R. B. Waghulde, M. G. Wankhede, "Ethanol vapour sensing properties of screen printed  $\text{WO}_3$  thick films", *Bull. Mater. Sci.*, Vol. 65, 2007, pp. 111-113.
3. T. Seiyama, A. Kato, K. Fujiishi, M. Nagatan, "A new detector for gaseous components using semiconducting thin films" *Anal. Chem.*, Vol. 34, 1962, pp. 1502-3.
4. S. Wolf, B. Nicolae, W. Udo, "Sensing of hydrocarbons and CO in low oxygen conditions with tin dioxide sensors: possible conversion paths", *Sens. Actuators B Chem.*, Vo. 103, 2004, pp. 362-368
5. U. Kreibig, M. Vollmer, *Optical Properties of Metal Clusters*, Springer Series in Material Science 25; Springer: Berlin, 1995.
6. L. Kelly, E. Coronado, L. Zhao, G.C. Schatz, "The Optical Properties of Metal Nanoparticles: The Influence of Size, Shape, and Dielectric Environment", *Phys. Chem. B*, Vol. 107, 2003, pp. 668-677.
7. C. Noguez, "The Influence of Shape and Physical Environment", *J. Phys. Chem. C*, Vol. 111, 2007, pp. 3806-3819.
8. P. V. Kazakevich, A. V. Simakin, V. V. Voronov, G. A. Shafeev, "Laser induced synthesis of nanoparticles in liquids", *Applied Surface Science*, Vol. 252, 2006, pp. 4373-4380.
9. Y. Zijie, D. B. Chrisey, "Pulsed laser ablation in liquid for micro-/nanostructure generation", *Journal of Photochemistry and Photobiology C: Photochemistry Reviews*, Vol. 13, 2012, pp. 204-223.
10. M. S. Tong, G. R. Dai, Y. D. Wu, D. S. Gao, "High sensitivity and switching-like response behavior of  $\text{SnO}_2\text{-Ag-SnO}_2$  element to  $\text{H}_2\text{S}$  at room temperature", *J. Mater. Sci.: Mater. Electron.*, Vol. 11, 2000, pp. 661-665
11. J. Li, Y. Wang, X. Gao, Q. Ma, L. Wang, J. Hang, " $\text{H}_2\text{S}$  sensing properties of the  $\text{SnO}_2$ -based thin films", *Sens. Actuators B*. Vol. 65, 2000, pp. 111-113
12. G. Blandenet, M. Court, Y. Lagarde, "Thin layers deposited by the pyrosol process", *Thin Solid Films*, Vol. 77, 1981, pp. 81-90
13. T. Okuno, T. Oshima, S. D. Lee, and S. Fujita, "Growth of  $\text{SnO}_2$  crystalline thin films by mist chemical vapour deposition method," *Physica Status Solidi C*, vol. 8, 2011, no. 2, pp. 540-542.
14. T. Mohanty, Y. Batra, A. Tripathi, and D. Kanjilal, "Nanocrystalline  $\text{SnO}_2$  formation using energetic ion beam," *Journal of Nanoscience and Nanotechnology*, Vol. 7, 2007, pp. 2036-2040
15. G. Neri, A. Bonavita, G. Rizzo et al., "Towards enhanced performances in gas sensing:  $\text{SnO}_2$  base nanocrystalline oxides application," *Sensors and Actuators B*, vol. 122, 2007, pp. 564-571.
16. K. S. S., Harsha *Principles of Physical Vapor Deposition of Thin Films*, Elsevier Science, Great Britain, 2006
17. M. Ganjali, M. Ganjali, S. Khoby, M. A. Meshkot, "Synthesis of Au-Cu nano-alloy

- from monometallic colloids by simultaneous pulsed laser targeting and stirring”, *Nano-Micro Letters*, Vol. 3, 2011, pp. 256-263
18. B. D. Cullity, *Elements of X-ray Diffraction*, 2<sup>nd</sup> Edition, Addison-Wesley, London, 1978.
19. X. Gao, G. Gu, Z. Hu, Y. Guo, X. Fu, “Simple Method for Preparation of Silver Dendrites” *Colloids and Surfaces A: Physicochemical Engineering Aspects*, Vol. 254, 2005, pp. 57 – 61
20. A. Hassanjani-Roshan, M. R. Vaezi, A. Shokuhfar, Z. Rajabali, “Synthesis of iron oxide nanoparticles via sonochemical method and their Characterization” *Particuology*, Vol. 9, 2011, pp. 95–99

